Development and performance evaluation of a prototype bio-optical sensor for in-water applications

by

Arshath Ramkilowan

BSc Hons(Phys)

Submitted in partial fulfilment of the requirement for

an MSc degree in the School of Physics, University of KwaZulu-Natal Pietermaritzburg

March 2012

Declaration

This thesis describes the work undertaken jointly at the University of KwaZulu-Natal and the Council for Scientific and Industrial Research (CSIR), under the supervision of Dr N.Chetty and co-supervision of Dr M.D. Lysko between February 2011 and February 2012.

I declare the work reported herein to be my own research, unless specifically indicated to the contrary in the text.

Signed: .....

On this..... day of 2012

I hereby certify that this statement is correct

.....
Dr N. Chetty
(SUPERVISOR)

.....
Dr M.D. Lysko
(Co-Supervisor)

Acknowledgements

First and foremost I would like to thank my supervisor Dr N Chetty and my co-supervisor Dr M.D Lysko. The faith in my ability you both have shown has moulded me into not only a better researcher, but a better person too.

The CSIR for funding my studies, without this assistance none of the research completed, experienced gained and opportunities offered would have been possible.

Dr S Bernard, the project leader of SWEOS, I am extremely grateful for both your assistance during field trials and the vast knowledge imparted to me.

To Ms Nobuhle Majozi and Mr Mark Matthews, I am especially thankful for your assistance in carrying out measurements during the Loskop field trial. Moreover, I'm glad to admit that your uninhibited enthusiasm for science has motivated and inspired me more than initially realised.

I would also like to express my deep gratitude and appreciation to Mr Bertus Theron and Mr Derek Griffith, for taking time to explain concepts, suggest ideas and for the guidance offered in general.

Last and certainly not least, to all my family, friends and loved ones, I thank you all for the courage, inspiration, support and morale boosting conversations. Your hand in completing this thesis has been most significant.

Table of Contents

1. Introduction

Eutrophication linked Harmful Algal Blooms[1] (HABs) are severely threatening the health of underprivileged rural communities through exposure to polluted waters. Livestock and marine mortalities in addition to quality non-compliance in agriculture and aquaculture sectors resulting from these unsafe waters has led to the loss of revenue, directly impacting on the country's economy.[2] Logistical and financial constraints hinder systematic and frequent monitoring of both saline and fresh national water ecosystems. A novel research initiative, Safe Waters Earth Observation Systems (SWEOS), aims to improve on current water monitoring schemes in South Africa by coupling satellite-based remote sensing procedures with low-cost autonomous in-situ radiometric sensor systems. Such a system offers cost effective, frequent, multi-scale and sustained observations using scalable techniques and technologies.[3]

Remote sensing is the science of acquiring information about an object without being in physical contact with that object. It has in recent years been widely utilised as a tool to probe the understanding of aqueous media (see for example, 4-6). Remotely sensed data is usually captured using instruments called radiometers. These devices resolve incoming electromagnetic radiation into component spectral bands, the finer the resolution the more detail there is extracted from the source of light (in this case, light reflected from a water body). Such instruments are typically mounted on platforms including satellites, aircrafts, ships or buoys.

Several successful attempts to capture water quality parameters in fresh water systems using sensors on board aircrafts have been reported (see for example, 7 and 8). While such a platform provides good spatial and spectral resolution it is the temporal inconsistencies and the high costs associated with this method in addition to the advent of satellite based remote sensing that make it less favourable to researchers in developing countries. The satellite remote sensing option provides the potential for time series data over several years or even decades (with the added option of using historic data). Successful

derivation of optical products for freshwater systems using imagery off satellite platforms have been achieved in literature (such as 9 and 10).

The atmospheric path separating a water body and satellite in addition to land masses adjacent to the water body both impact on the interpretation of the signal received by the satellite sensor. Both adjacency[11] and atmospheric effects[12, 13] can however be addressed by using radiative transfer algorithms, a field on its own and currently beyond the scope of this research.

Satellite derived optical products must be validated with in-situ water truth data to test the efficiency of the radiative transfer algorithms. For this to be achieved; accurate, reliable and robust in-situ radiometers moored independently or mounted on buoys are required. These devices are also often used to capture data needed for the development of the aforementioned corrective algorithms. Several commercially available sensor options exist from manufacturers such as Wetlabs Inc, TriOS Optical Sensors, Satlantic Inc and Ocean Optics Inc.

The work presented in this thesis, includes two scientific papers (submitted for publication) focusing on the design, development and performance evaluation of a first generation prototype autonomous bio-optical sensor. The radiometer is named Hyperspectral Device for Radiometric Observations in Water (HyDROW). The purpose of HyDROW includes, but is not limited to; water constituent monitoring, satellite calibration validation and ocean colour satellite product corroboration.

The confidence of the validation process increases as the number of validation sites increase, especially for turbid water ecosystems where the optical behaviour of the water has significant variation. Ship based in-situ validation offers spatial coverage that can maximise confidence of the validation process. Paper 1 of this thesis briefly outlines the shortcomings of this method and suggests the deployment of several independently moored or buoyed systems to create multiple validation sites. Most of the commercially available instruments capable of achieving this are often unfeasible for purchasing in bulk; as a result the need for development of cost-effective

radiometric technology with minimal compromise on performance is identified, and consequently addressed in this research. The focus of paper 1 is on the decision making processes involved in the development of the autonomous bio-optical sensor whose purpose includes (but is not limited to): water constituent monitoring, satellite calibration validation and ocean colour satellite product matchups. Paper 1 was submitted to the South African Journal of Science on January 31, 2012 and is currently under review.

Paper 2 reports on the performance of HyDROW based on observations in an optically diverse water basin and by comparison against a reliable commercial instrument. Paper 2 was submitted to the Journal of Atmospheric and Oceanic Technology on February 11, 2012 and is currently under review.

Finally, in addition to its envisaged satellite validation capability, a realised network of HyDROWs can be used as an early warning bloom detection and in-water monitoring system. Such an instrument also has the advantage of being deployed in remote, high priority areas that are inaccessible to boat or satellite measurement acquisition.

2. Research Strategy

The flowchart in figure 1 illustrates the manner in which the research was and continues to be addressed for the sensor development facet of SWEOS. HyDROW has been designed, lab tested, packaged, re-lab tested and field tested. The positive results from the performance test during the field campaign (see paper 2) suggest that minor improvements are needed to increase confidence on the data collected with HyDROW.

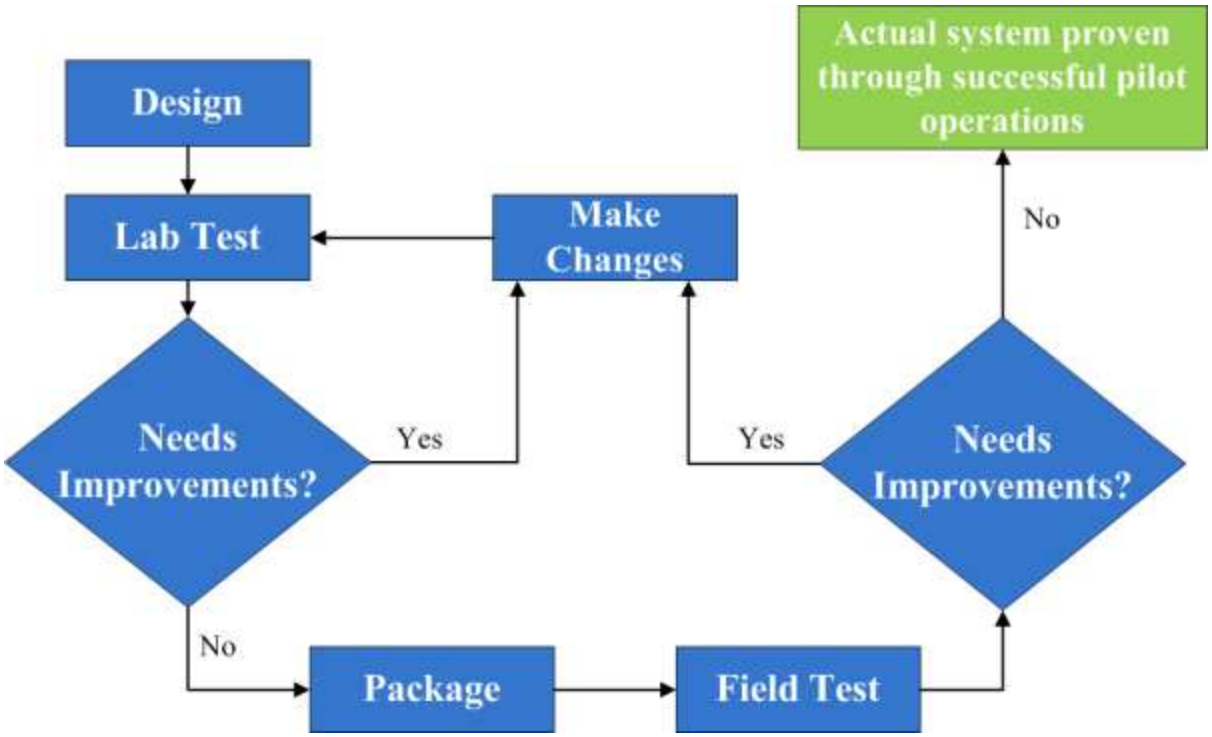

Figure 1 Flowchart for research strategy

3. Radiometry of HAB detection

One of the primary goals of optical oceanography and limnology is to understand how the behaviour of underwater light influences and is influenced by the ecology of the aquatic ecosystems. The relationship that exists between optical properties and the biological, chemical and geological constituents of natural waters define the crucial function of optics in aquatic research.[14] To recognise the underlying physical principles that govern this relationship and the fate of electromagnetic radiation upon its interaction with water bodies and the inhabiting organic constituents, fundamental radiometric terminology need be introduced.

3.1. Solid Angle

Solid angle is a three dimensional extension of a planar angle, whose magnitude at a point P is determined by an area A, projected onto a sphere centered at P, divided by the radius r of the sphere.

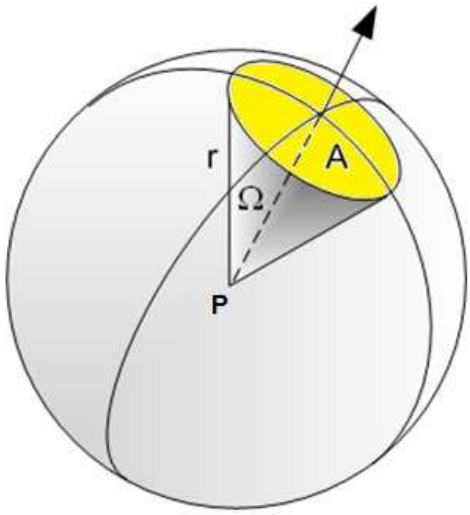

- $\omega = \frac{A}{r^2} \qquad (sr)$

Figure 2 Pictorial description of solid angle

3.2. Radiance

Radiance can be defined as the density of flux over a source surface area and solid angle with the flux flowing in an outward direction perpendicular to the surface area.

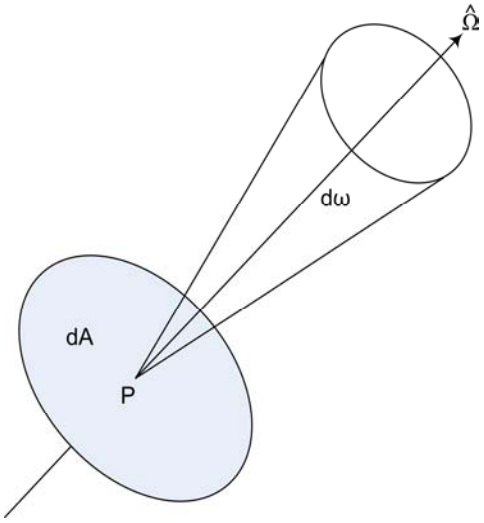

- $L = \frac{d^3Q}{dA \cdot d\omega \cdot dt}$ $\left(\frac{W}{m^2.\ sr}\right)$
- d^3Q is the differential energy
- dA is the infinitesimal Source area
- $d\omega$ is the infinitesimal solid angle
- $\hat{\Omega}$ is the flux flow direction

Figure 3 Graphical description of radiance

Typically it is necessary to express the amount of radiation at each wavelength, i.e. spectral radiance. This is given by,

$$L_\lambda = \frac{d^3Q}{dA \cdot d\omega \cdot dt \cdot d\lambda} \tag{1}$$

where the subscript λ denotes that the radiance depends on λ and the interval in λ.

3.3. Irradiance

Irradiance is usually defined as the density of flux over a receiving area, with the flux flowing in an inward direction.

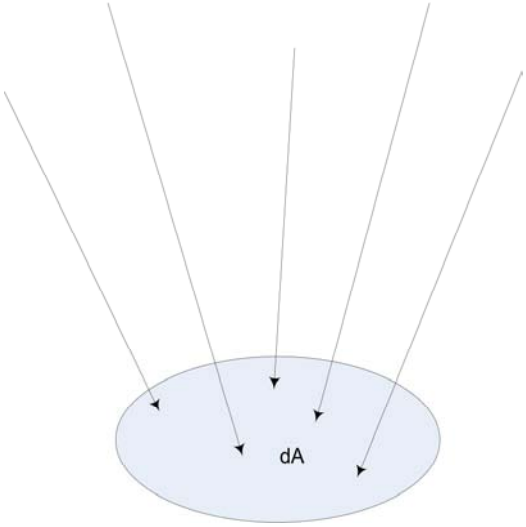

- $E = \frac{d^2Q}{dA \cdot dt}$ $\left(\frac{W}{m^2}\right)$
- d^2Q is the differential energy
- dA is the receiving area

Figure 4 Graphical description of irradiance

Analogous to spectral radiance, spectral irradiance is irradiance in a differential wavelength interval dλ, centered at a specific wavelength λ is given by

$$E_\lambda = \frac{d^2Q}{dA \cdot dt \cdot d\lambda} \tag{2}$$

3.4. Spectral Region of Interest

The Sun is a source of energy across the electromagnetic spectrum. Moreover, the Sun and earth coupling is responsible for atmospheric and biological processes on earth. The portion of the electromagnetic spectrum that is pertinent to the research presented in this thesis is defined as being between 400 nm and 750 nm (the visible spectrum), since:

1) The black body emission spectrum of the Sun, plotted in Figure 5 by using Planks law (equation 3), is contained predominantly between 300 nm and 2500 nm. As the radiation traverses the atmosphere, energy in certain spectral bands undergoes significant attenuation. Figure 6 is an illustration of the solar irradiance at the top of the atmosphere (TOA) and at the Earth's surface. The differences between the two spectra are a result of atmospheric absorption and scattering.

$$B_\lambda(T) = \frac{2hc^2}{\lambda^5} \cdot \frac{1}{e^{\frac{hc}{\lambda k_B T}-1}} \tag{3}$$

- $B_\lambda(T)$, is the wavelength dependant spectral radiance and T is the absolute temperature in Kelvin
- h, is Plancks constant = 6.626 x 10^{-34} Js^{-1}
- k_B, is the Boltzmann constant = 1.380 x 10^{-23} JK^{-1}
- c, is the speed of light in a vacuum = 2.998 x10^{8} ms^{-1}

The inherent structure of water makes water a strong absorber of red and infrared light, thus setting a realistic upper limit of 750 nm.

2) The spectra obtained for in-water upwelling radiance will be altered due to the absorption and scattering of constituent particles, both organic and inorganic. Absorption and scattering features of certain particles act as a unique signature, often assisting one in identifying the type of substance present in the water mass and its relative concentration. This is demonstrated in figures 7 and 8 where unique

absorption features of chlorophyll pigments alter the natural solar spectrum in a distinctive manner. The absorption bands cause a drop in photon count at the wavelengths of absorption. It is this feature that can be used to identify the particles.

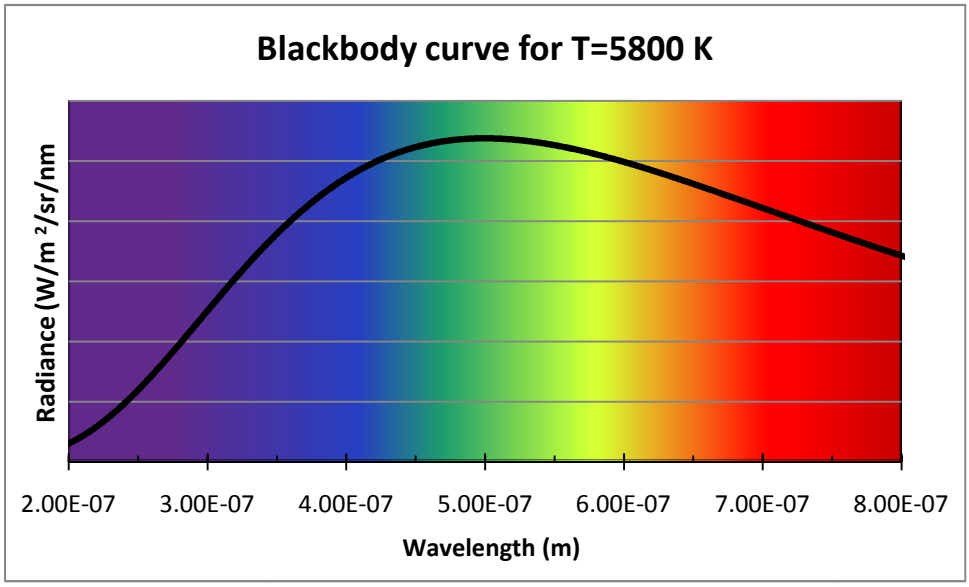

Figure 5 Blackbody curve approximating the radiance spectrum of the Sun

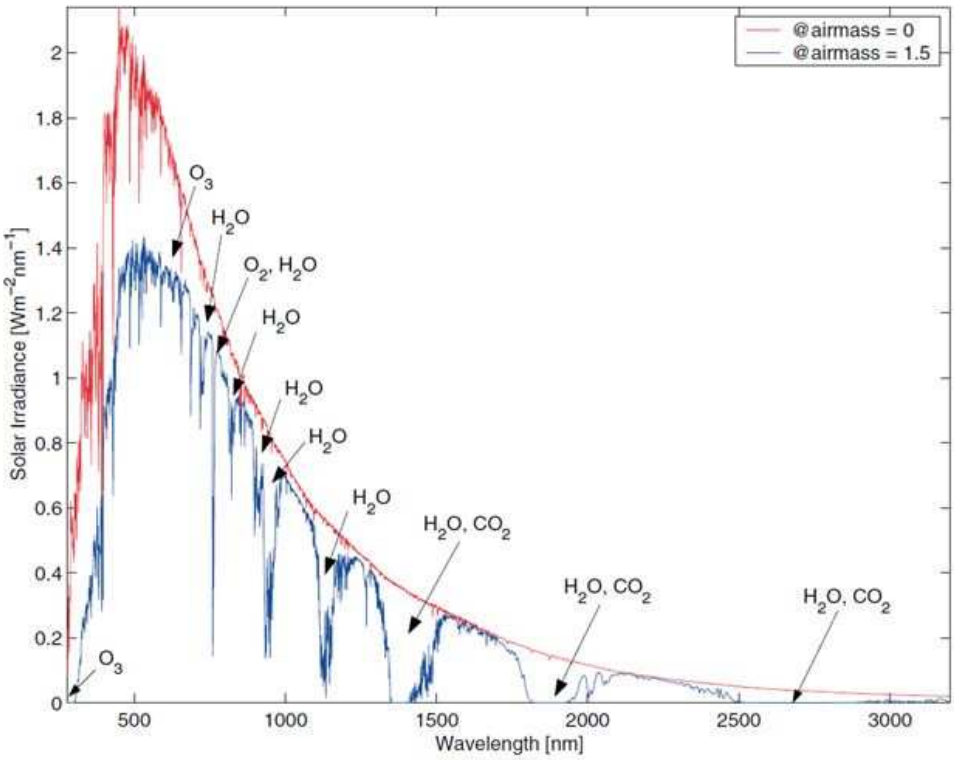

Figure 6 Solar irradiance at TOA[15] and Surface of the Earth[16]

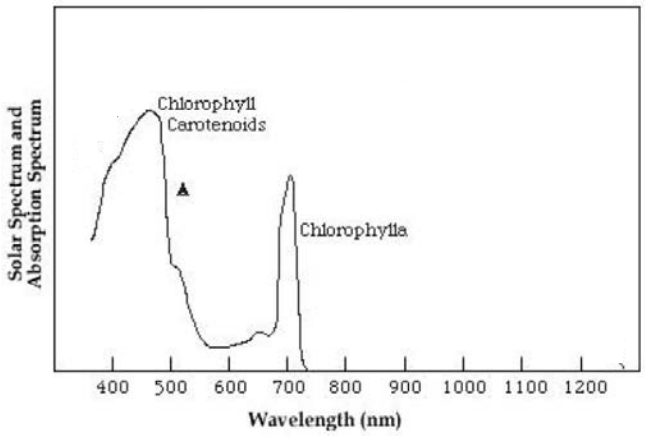

Figure 7 Absorption spectrum of Chlorophyll [17]

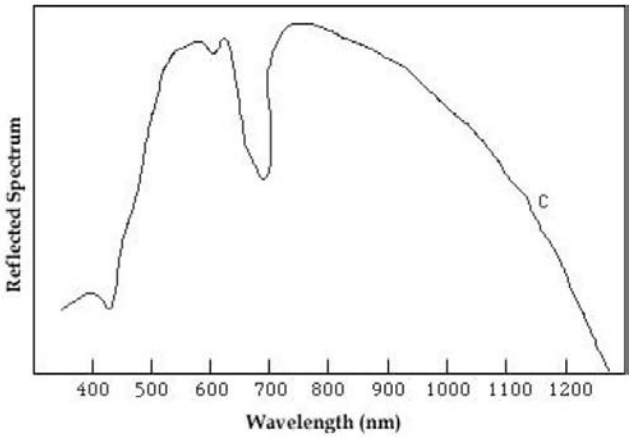

Figure 8 The reflectance spectrum of Chlorophyll[17]

4. Upwelling radiance in retrieving satellite remote sensed data

Complete and accurate upwelling radiance measurements at some depth z below the surface of a bulk water-mass are highly sought after in areas of science including remote sensing, limnology and oceanography amongst others. Such measurement values are used in the determination of remote sensing reflectance, (R_{rs}) and normalised water leaving radiances, (L_{WN}). Both of which are used as input values into algorithms designed for deriving a host of optical properties that provide insight into the identity and concentration of in-water constituents of the target water body; chlorophyll content, spectral volume absorption coefficients to name a few.

The following two subsections define the parameters R_{rs} and L_{WN} as used in remote sensing for water monitoring. The discussion is based on the illustration given in figure 9.

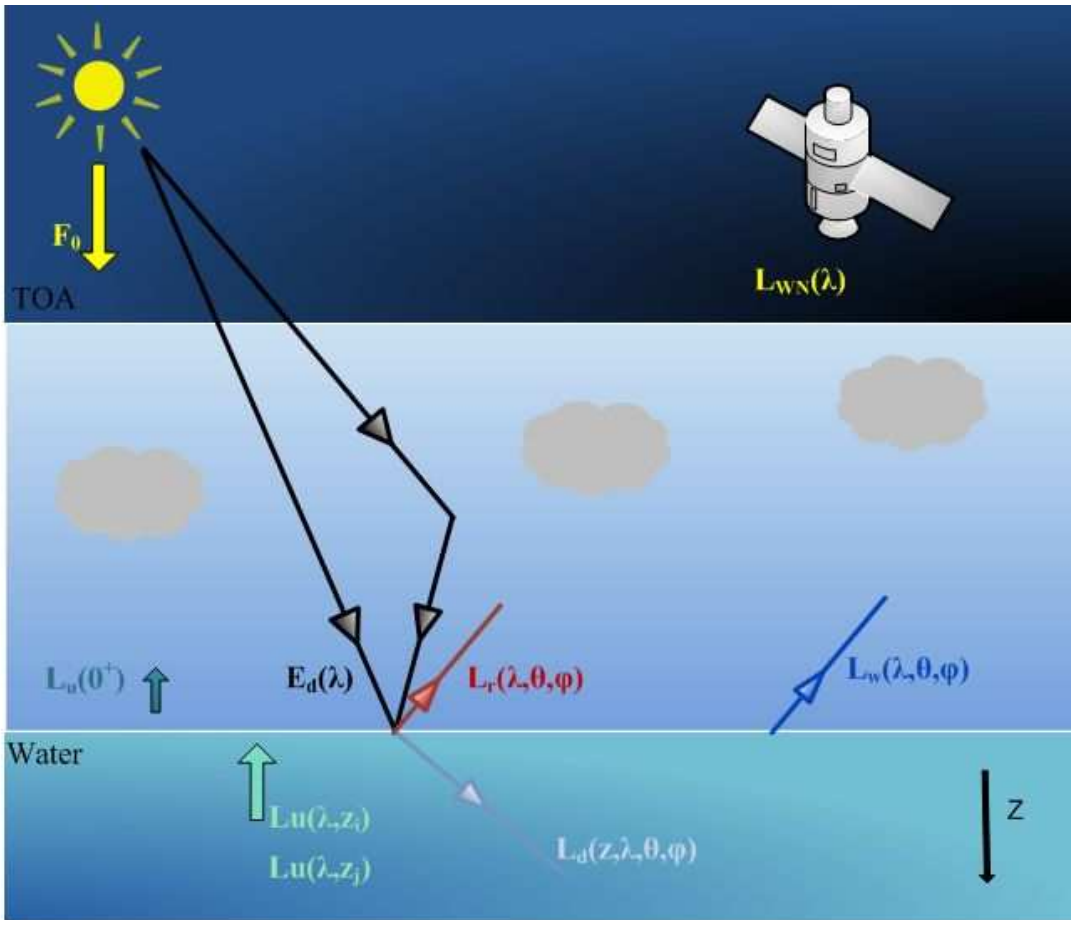

Figure 9 Fate of light during satellite based remote sensing

4.1. Remote sensing reflectance R_{rs}

Remote sensing reflectance is a parameter regularly employed with satellites to obtain information on the constituents present in a given water body. It is defined as the measure of downwelling irradiance incident on the water surface that is returned back through the surface into some infinitesimal cone of acceptance centered on nadir and azimuthal angles θ and ϕ respectively, as defined below (in equation 4).[14]

$$R_{rs} \equiv \frac{L_w(\theta, \phi, \lambda)}{E_d(\lambda)} \tag{4}$$

Here both L_w, the water leaving radiance and E_d, the total downwelling irradiance (contributions from sun and sky) are evaluated in air (just above the air-water interface). L_w in (equation 4) cannot be directly measured. It is inferred via one of two methodologies, each having arguments for and against its favoured use, as discussed in (18 and 19).

The first method for estimating the water leaving radiance requires an estimate of the surface-reflected radiance L_r, which in itself cannot be directly measured. Subtracting L_r from a measurement of the upwelling radiance just above the water surface $L_u(0^+)$ leaves an estimate of the water leaving radiance as indicated from equations (4) and (5).

$$R_{rs} = \frac{L_u(0^+) - L_r}{E_d(\lambda)} \tag{5}$$

The second method requires a measurement of the upwelling radiance at a fixed depth (preferably several fixed depths). Measurements below the surface are then extrapolated through the water column to the water surface to give the L_w estimate shown in (6).[20]

$$R_{rs} = \frac{t}{n^2}\frac{L_u(z_i,\lambda)}{E_d(\lambda)}e^{K_L(\overline{z_{ij}},\lambda)z_i} \quad (6)$$

Where $\overline{z_{ij}}$ is the average of depths z_i and z_j as indicated in Figure 9, t is radiance transmittance of the surface and n^2 is the real refractive index of the water. K_L is the diffuse attenuation factor for upwelling radiance.

4.2. Normalised water-leaving radiance L_{WN}

Normalized water-leaving radiance, often used for satellite validation protocols is approximately the radiance that would exit the ocean in the absence of the atmosphere, with the sun at zenith, at the mean earth-sun distance (1 AU). It is given by,

$$L_{WN} = L_w \cdot \frac{F_o}{E_d} \quad (7)$$

where F_0 is the mean extraterrestrial solar irradiance.

5. Summary

The need for a powerful, cost effective and robust method of addressing algal bloom related hazards has been identified. The Safe Waters Earth Observation System (SWEOS) initiative aims to address this need. An invaluable element of project SWEOS is the development of autonomous cost effective, bio-optical sensors. Consequently, two candidate spectrometer cores were experimentally examined with the aim of integrating the best performing detector into a prototype radiometric device. Several strategically chosen criteria were used, along with a set of compromises that were necessarily made in order to meet the cost-effective-high-performance mandate set out by project SWEOS. The CMOS detector selected for integration into the radiometric system, HyDROW, was found to be the superior module for this particular application, with regard to both cost and performance.

To test the performance of the prototype instrument in an uncontrolled environment it was taken to Loskop Dam in the Mpumalanga province of South Africa. Measurements were made with HyDROW and a reference radiometer, HyperTSRB, at 5 optically dynamic sites. The variation in turbidity between these sites was highly uncommon, and resulted in the HyDROW been tested across its entire dynamic range. This helped conclude an unbiased performance assessment of the instrument. Correlation co-efficients were greater than 0.99 with the exception of the most turbid site visited, where an $r = 0.97$ was recorded. The variation in data measurements of the reference radiometer for this site was high which indicates that the 0.97 is reasonable. Percentage differences between HyDROW and HyperTSRB were calculated and found to be at most 30% but on average less than 20 %. It is expected that post processing corrective measures such as accounting for stray-light effects and self shadowing contributions to the uncertainty budget, will significantly lower the relative error difference.

The results indicate that HyDROW proof of concept has been achieved. The instrument is not yet ready to be used as a satellite validation tool, but

results advocate wholly that should HyDROW be produced in larger numbers with the added capability of near real-time data acquisition, then it can indeed provide as an early warning bloom detection and water monitoring network.

The success of HyDROW has spurred the design and development of an irradiance sensor as well as a second more ambitious, first of its kind prototype, that in theory can deliver radiance, backscatter and fluorescence measurements. This second prototype is to be deployed at Saldanha Bay on South Africa’s west coast for a two month period with the aim of evaluating its performance relative to a TriOS radiometer.

6. References

[1] Eutrophication Monitoring Guidelines by Remote Sensing for the NOWPAP Region, NOWPAP Special Monitoring & Coastal Environmental Assessment Regional Centre (NOWPAP CEARAC), 2007.

[2] Bernard S. Research proposal on Safe Waters Earth Observation Sytems (SWEOS), CSIR, 2010 (Unpublished report)

[3] Bernard S., R. Kudela, P. Franks, W. Fennel, A. Kemp A. Fawcett and G.C. Pitcher. 2006. “Part III, Chapter 12: The requirements for forecasting harmful algal blooms in the Benguela,” In THE BENGUELA :PREDICTING A LARGE MARINE ECOSYSTEM. Large Marine Ecosystems. ISBN-13: 978-0-444-52759-2,Elsevier, 438 pages

[4] CHANG, K.W., SHEN, Y. and CHEN, P.C., 2004. Predicting algal bloom in the Techi reservoir using Landsat TM data. International Journal of Remote Sensing, 25(17), 3411-3422.

[5] THIEMANN, S. and KAUFMANN, H., 2000. Determination of chlorophyll content and trophic state of lakes using field spectrometer and IRS-1C satellite data in the Mecklenburg lake district, Germany. Remote Sensing of Environment, 73(2), 227-235.

[6] VINCENT, R.K., QIN, X.M., MCKAY, R.M.L., MINER, J., CZAJKOWSKI, K., SAVINO, J. and BRIDGEMAN, T., 2004. Phycocyanin detection from LANDSAT TM data for mapping cyanobacterial blooms in Lake Erie. Remote Sensing of Environment, 89(3), 381-392.

[7] HAKVOORT, H., DE HAAN, J., JORDANS, R., VOS, R., PETERS, S. and RIJKEBOER, M., 2002. Towards airborne remote sensing of water quality in The Netherlands—validation and error analysis. ISPRS Journal of Photogrammetry and Remote Sensing, 57(3), 171-183.

[8] KOPONEN, S., PULLIAINEN, J., KALLIO, K. and HALLIKAINEN, M., 2002. Lake water quality classification with airborne hyperspectral spectrometer and simulated MERIS data. Remote Sensing of Environment, 79(1), 51-59.

[9] FLORICIOIU, D., ROTT, H., ROTT, E., DOKULIL, M. and DEFRANCESCO, C., 2004. Retrieval of limnological parameters of perialpine lakes by means of MERIS data, H. LACOSTE and L. OUWEHAND, eds. In: Proceedings of the 2004 Envisat & ERS Symposium (ESA SP-572), 6 - 10 September, Salzberg, Austria, 2004, ESRIN-ESA pp1-5.

[10] GIARDINO, C., CANDIANI, G. and ZILIOLI, E., 2005. Detecting chlorophyll-a in Lake Guarda using TOA MERIS radiances. Photogrammetric Engineering & Remote Sensing, 71(9), 1045-1051.

[11] BRANDO, V.E. and DEKKER, A.G., 2003. Satellite hyperspectral remote sensing for estimating estuarine and coastal water quality. IEEE Transactions on Geoscience and Remote Sensing, 41(6), 1378-1387.

[12] SONG, C., WOODCOCK, C., SETO, K.C., LENNEY, M.P. and MACOMBER, S.A., 2001. Classification and change detection using Landsat TM Data- When and how to correct atmospheric effects? Remote Sensing of Environment, 75(2), 230-244.

[13] VIDOT, J. and SANTER, R., 2005. Atmospheric correction for inland waters-application to SeaWiFS. International Journal of Remote Sensing, 26(17), 3663-3682.

[14] Ocean Optics Web Book, http://www.oceanopticsbook.info/view/overview, accessed on 2 February 2012.

[15] Gueymard C., Myers D., Emery K., Proposed Reference Irradiance Spectra for Solar Energy Systems Testing, Solar Energy, Vol. 73, Issue 6, pp. 443- 467, December 2002.

[16] Gueymard C.A., The Sun's Total and Spectral Irradiance for Solar Energy Applications and Solar Radiation Models, Solar Energy, 76, pp. 423-453, 2004.

[17] Environmental Decision Making, Science, and Technology, http://telstar.ote.cmu.edu/environ/m3/s2/02sun.shtml, Accessed on 11 February 2012

[18] O'Reilly, J.E., S. Maritorena, B.G. Mitchell, D.A. Siegel, K.L. Carder, S.A. Garver, M. Kahru, and C. McClain. 1998. Ocean chlorophyll algorithms for SeaWiFS. J. Geophys. Res. 103(C11), 24937-24953.

[19] Mobley, C.D., L.K. Sundman, C.O. Davis, J.H. Bowles, T.V. Downes, R.A. Leathers, M.J. Montes, W.P. Bissett, D.D.R. Kohler, R.P. Reid, E.M. Louchard, and A. Gleason. 2005. Interpretation of hyperspectral remote-sensing imagery by spectrum matching and look-up-tables. Appl. Optics 44(17), 3576-3592.

[20] Chang G.C, Tommy D. Dickey, Curtis D.Mobley, E. Boss, W.S. Pegau., 2003. Towards closure of upwelling radiance in coastal waters. Optical Society of America, Applied Optics, Vol. 42, Issue 9, pp. 1574-1582.

Paper I

Optical Detectors for Integration into a Low Cost Radiometric Device for In-Water Applications: A Feasibility Study

A. Ramkilowan, Dr N. Chetty, D.J. Griffith, Dr M.D. Lysko

Submitted to the South African Journal of Science (31 January, 2012), and printed herein according to the submission guidelines suggested by the Journal editors.

Optical Detectors for Integration into a Low Cost Radiometric Device for In-Water Applications: A Feasibility Study

ABSTRACT

Higher water temperatures and nutrient loads, along with forecasted climate changes are expected to result in an increase in the frequency and intensity of eutrophication-linked algal blooms.[1] The destructive impact such phenomena have on marine and freshwater systems threaten aquaculture, agriculture and tourism industries on a global scale.[1] An innovative research project, Safe Waters Earth Observation Systems (SWEOS) proposes the use of space-based remote sensing techniques, coupled with in-situ radiometric technology to offer a powerful and potentially cost effective method of addressing algal bloom related hazards. The work presented in this paper focuses on the decision making processes involved in the development of autonomous bio-optical sensors whose purpose includes, but is not limited to; water constituent monitoring, satellite calibration validation and ocean colour satellite product matchups. Several criteria including optical throughput, linearity and spectral sensitivity were examined in an attempt to choose the detector best suited for its intended application. The CMOS based module tested in the laboratory experiments was found to have produced the best performance at the lower price and was subsequently chosen for integration into the in-water radiometric device built and tested at the CSIR.[2] Mass production of this prototype technology will commence, pending data quality comparable to that of an already calibrated, in-water radiometer; to be tested at field trials in Elands Bay, Loskop and Saldanha Bay.

INTRODUCTION

The growth of microscopic algae (called phytoplankton) is imminent as the organic content within a water body or region thereof increases. Despite the minute size of these organisms, their numbers have the potential to grow very rapidly. This explosive increase in phytoplankton biomass is dubbed a bloom. When the species of algae in the bloom cause detrimental effects to the ecosystem they inhabit, they are labeled harmful algal blooms, commonly referred to as HABs in the limnology and marine science communities. Detail on the environmental and economic impacts of HABs is discussed in detail by multiple authors. [5-7] The large scale impact HABs have on the environment drives the need for a forecasting system that helps to facilitate corrective measures and treatment procedures of affected waters[2]. The heterogeneous nature of the oceans coupled with non-trivial bloom dynamics necessitates that such a system have the required data captured at a high temporal frequency on as large a spatial scale as possible. Satellite imagery aptly satisfies these two requirements and has for the last few decades been the best tool for such initiatives.[8-10]

To better understand satellite measurements and their inherent uncertainties, it is necessary to calibrate and validate such spaceborne data. This requires in-situ radiometric measurements to be captured almost simultaneously with those acquired on board satellites. For an accurate and reliable inter-comparison the in-situ data obtained needs to have an appropriately high spatial distribution. A study conducted by the NOWPAP research group[11] suggests a minimum of 10 in-situ sampling points per satellite measurement separated by a distance dependant on the satellite spatial resolution (250 – 500m). As a result the method often employed for capturing in-situ data for calibration and validation activities is ship-based. However, regular, continuous and time-specific measurements via this method of monitoring are costly and or not always possible. The inability to access remote areas provides an added disadvantage. Hooker and McClain[12] as well as Cullen and Ciotti[13] discuss the future possibilities of basic cost effective and light-weight instrumentation as the optimal manner for gathering accurate and reliable sea-truth data. Such devices, if able to produce high quality data,

would be moored at a large number of strategic locations resulting in a spatial coverage equal to or better than that offered by any other in-situ monitoring method.

Development of low-cost radiometric instrumentation for in-water applications without jeopardising performance requires careful considerations and innovative compromises. The sections that follow herein give an overview of the decisions made in choosing the sensor to be used in the prototype radiometer. An experimental, quantitative and where necessary graphical discussion outlining the capabilities of two short-listed spectrometer cores precedes a brief summary of the research completed. The paper concludes with a justification for the choice of sensor, and a mention of future endeavours planned using the resulting radiometric device.

BACKGROUND

The SWEOS project is a multi-disciplined initiative seeking to address the severe impact HABs have on water resources in South Africa as is documented by Oberholster and Ashton.[14] The project combines an innovative ensemble of remote sensing techniques with robust, cost effective and autonomous in-situ technology. The primary use for this Earth Observation (EO) system is to provide a means for monitoring water quality in high impact coastal and inland water bodies.[1]

An invaluable facet of project SWEOS is the development of economically priced radiometric sensors. Deploying large numbers of these bio-optical instruments creates a network of sensors providing the ability to thoroughly characterise ecosystems by validating the pertinent satellite derived data. The sensor network also has the potential to act as an early warning bloom detection system, the need for which has been addressed by Oberholster and Claasen[15] for inland water bodies and Hutchings and Roberts[16] for coastal ecosystems.

The SWEOS mandate places low-cost as the largest driving factor for the envisaged technology. The target is to realise a system with market potential at less than 50 % the price of present commercial systems. The spectrometer

core has the largest impact on cost and performance. As a result the selection of an appropriate detector has been prioritised.

A report compiled by Lysko and Griffith[17] found that two OEM sensors closely met the pre-defined selection criteria and may be the best suited candidates for integration into the radiometric device. Both the shortlisted candidates (hereafter referred to as C1 and C2) have an architecture incorporating a tightly knitted optical input and spectral dispersion mechanism. This proved advantageous as it could be easily incorporated into the intended light-weight, compact and autonomous design.

SENSOR DESCRIPTION

Architecture

Commercial ocean colour radiometers have evolved from the somewhat limited single channel detector type spectrophotometers, seen for example in Choi[18] and Robertson[19]. The current conventional ocean colour systems realise multiple channels with a silicon photodiode array, CCD array or a CMOS array. In all cases, the broad-band light source is diffracted by a dispersing element onto an imaging sensor, made up of tiny photosites (pixels). The light sensitive pixels absorb incident photons and release electrons through the photoelectric effect.[20] The accumulation of charge over the exposure time is transferred and converted to an analogue voltage which is subsequently converted into a digital number. The entire image is now a collection of numbers that can be manipulated to give the spectral signature of the source under study.

Sensors C1 and C2 employ the CMOS linear array architecture which differs from the CCD detectors (commonly found in digital cameras) only in the manner by which the charge is transferred and where it is converted to a voltage.

Optical design

The influence optics has on the fate of the light entering the system is illustrated in figure 1 for C1 and C2.[21] The optical design of C2 takes on a more conventional approach in which the light entering through a restricting

slit is collimated onto a grating and the resulting spectrum focused onto the image sensor. The compactness of C1 is as a result of a coupling of the collimating and dispersing mechanisms. This is achieved by imprinting a diffraction grating onto a focusing lens. The latter offers the flexibility of a high spectral resolution within a miniaturised spectrometer head. This is an advantage for applications demanding light weight and compact payloads.

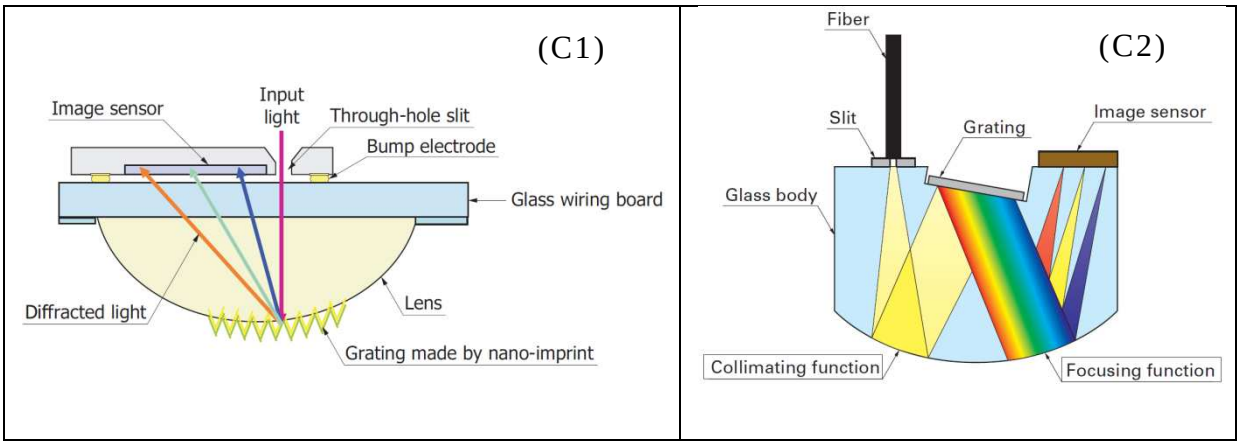

Figure 2: Input Light Relay for C1 and C2[21]

FIGURES OF MERIT

In order to quantitatively describe and compare the performance of C1 and C2, certain figures of merit have been considered. These include: spectral ran ge, spectral sensitivity, spectral res-olution, optical throughput and the Signal-to-Noise Ratio (SNR).

Spectral range and response

The portion of the electromagnetic spectrum that is pertinent to most in-water measuring applications ranges from 400 nm to 750 nm. Choosing a detector with sufficiently high spectral sensitivity in this region is therefore a prerequisite. Both short-listed sensors, C1 and C2, are sufficiently sensitive within the required spectral window.

The plots in Figure 3, as taken from relevant specification sheets [21, 22] give the relative spectral sensitivity for C1 and C2. It is desirable to have a smooth and flat spectral response to reduce uncertainties related to spectral

binning. C1 has a higher sensitivity as well as a smoother and more flat spectral response in the 400 nm to 750 nm region of interest, giving it a distinct and considerable advantage over C2.

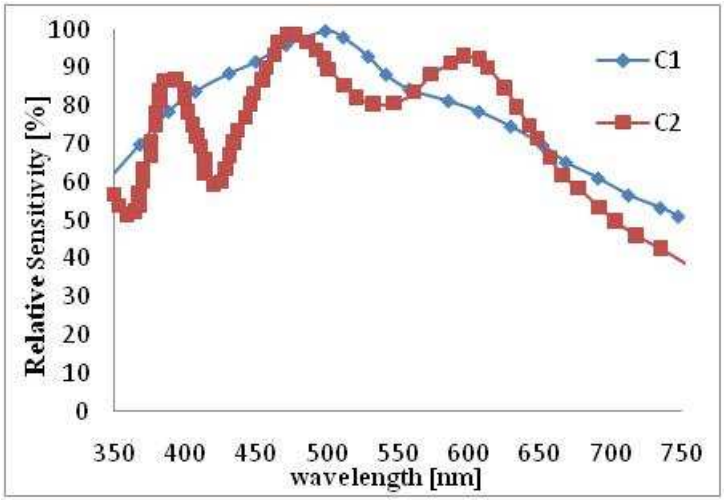

Figure 3: Typical Relative Spectral Sensitivity at 25°C Ambient Temperature

Spectral resolution

The spectral resolution offered by C1 and C2 are 10 nm[23] and 12 nm[21] respectively. These resolutions are considered to be ample for capturing the upwelling radiance in water, which usually exhibits spectral signatures devoid of sharp features, as seen in work completed by Ramkilowan and Chetty[2], Dierrsen and Kudela[7] as well as Kohler and Philpot.[22] The improved resolution (by 2 nm) that C2 has over C1 is insignificant to this application.

Optical Throughput

Highly turbid waters will result in low upwelling radiances which may impinge on the detectivity of the sensor. Such scenarios may be avoided by optimising geometric coupling between the light source and the detector so as to maintain optical throughput. By definition, the optical throughput G is an indication of the total flux that can pass through a system and is the product of the maximum cone of flux received at the slit entrance and the sensitive slit area.

$$G = \pi \sin^2(\theta).s, \qquad \text{equation (1)}$$

The slit areas for C1 and C2 are the areas of the through-hole-slit and slit in the respective diagrams of Figure 1. Clearly, *G* may be increased by increasing *s*. The slit width is nominally fixed and is pre-defined by the dispersive optics and the spectral resolution requirements. With assumption of an appropriate choice of slit width, an increase in slit height may increase stray light and also reduce resolution and bandpass. This will result in an increase in system aberrations. The entrance slit dimensions, as provided by the manufacturers, are 75 μm (height) x 750 μm (width) for C1 and 50 μm x 300 μm for C2.[21, 22] Given that C1 and C2 have the same acceptance solid angle, then from equation (1) it is inferred that C1 has the larger sensitive slit area and thus the greater optical throughput. One may expect that this is with a compromise with respect to stray-light and resolution.

Sensor Noise and Stability

From prior observations, the in-water upwelling radiance levels that are expected to be encountered will result in exposure times for a detector ranging from 0.05 seconds for oligotrophic waters, to 2 seconds in hypertrophic waters.[6]

A programmable system allows for exposure time adjustments and ensures that the signal acquired makes use of as much of the dynamic range as possible while avoiding pixel saturation. In this way acceptable levels of signal-to-noise ratio (SNR) are maintained.

A thorough characterisation of the SNR requires consideration of several contributing factors, among those being photon shot noise, dark signal noise, readout noise and digitization noise. For this research the total system noise was considered instead; an estimate of the total system noise is given by the standard deviation of an accumulation of repetitive measurements. The SNR for C1 and C2 was then calculated by normalising the central tendency to the standard deviation of a given data set. It is noted that for a uniform light source, such as the one employed during this experiment, the central tendency should be inferred using the mean of the sample set, whereas the

median should be used for a light source susceptible to outliers, such as that encountered during field measurements.

The SNRs have been investigated from measurements with C1 and C2 in the laboratory using a spatially uniform blue-green light emanating from an integrating sphere having a 25 cm diameter. A spatially uniform input radiance is necessary to reduce uncertainties associated with detector non-uniformity. The light source chosen was an approximation of the upwelling spectral radiance measurements expected for ocean based observations.

A layout for the laboratory test is given by Figure 4, where the horizontal translation refers to the ability to shift modules C1 and C2 horizontally so as to have the same central position during data acquisition. The SNR for C1 and C2 (both relative to the maximum SNR for C1 and based on a set of 10 samples per sensor at a 50 ms exposure time) is shown in the plots of Figure 5. The relative comparison of SNR for the two candidates indicates that C1 has a superior SNR across the entire visible spectrum.

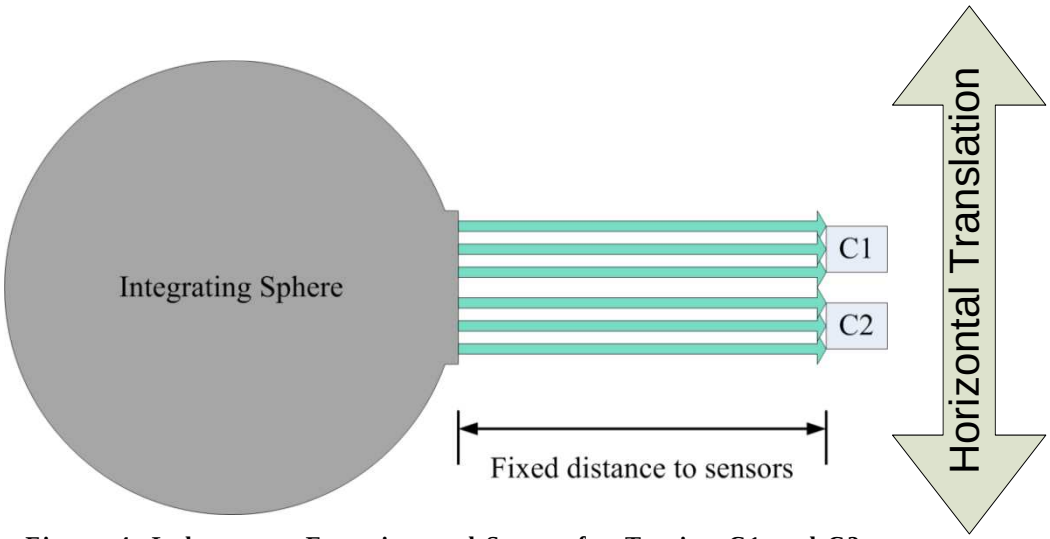

Figure 4: Laboratory Experimental Set-up for Testing C1 and C2

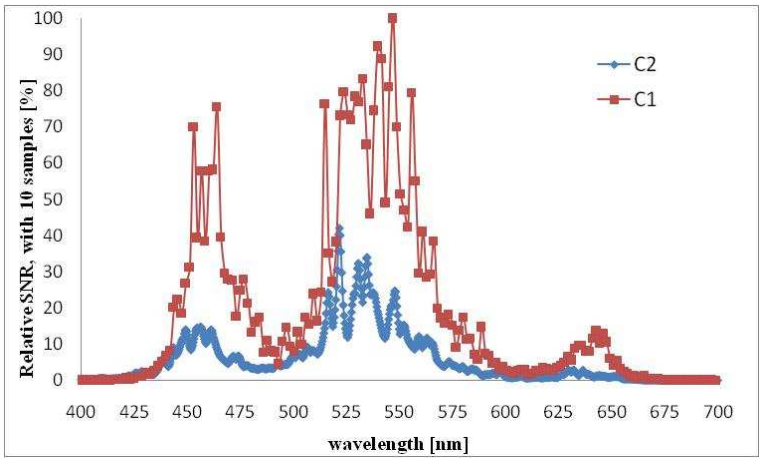

Figure 5: Normalised SNR for Sample Size = 10

MINIMISING ERRORS

For the low-cost mandate to be adhered to, the choice of candidate sensors lacked features present in some high precision commercial instruments. As a result, the performance of the prototype radiometer would be compromised. While not every feature that lends itself to the high cost of commercial ocean colour radiometers can be accurately catered for; a concerted effort was made to minimise the errors most likely to have a significant impact on quality of data. Factors that were considered but compromised on include temperature stability of the instrument, capacity to acquire dark signal measurements and correction for stray light.

Linearity

Stray light plays a major role in the non-linear behaviour of the candidate radiometric modules. While the departure from linearity (figure 5) is not ideal, sacrificing good stray light correction for low cost was a necessary compromise. The disadvantage of the minimal stray light corrections (if any) offered by the manufacturer is reasonably catered for in an experiment conducted by Ramkilowan and Chetty.[2]

Laboratory measurements using the set-up as in Figure 3 were taken at incremental exposure times to determine the linearity of the two sensors at a selected few wavelengths. The wavelengths were chosen so as to coincide with typical optical bands of sensors onboard ocean colour satellites.

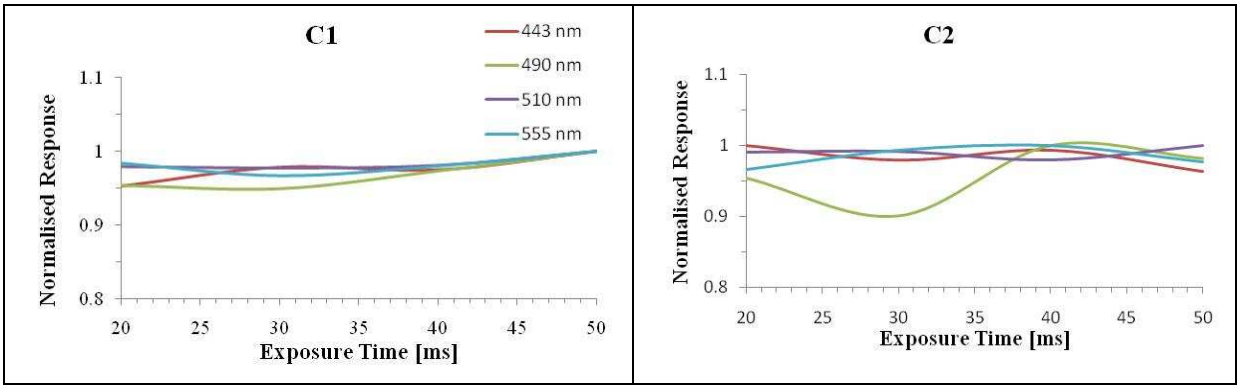

Figure 6: Linearity with respect to Exposure Time

Temperature control of detector

The benefits of a temperature controlled sensor have long since been established;[25] however the autonomous nature of the in-situ instruments provides a low power constraint. It is therefore necessary to forego cooling of the sensor and to calibrate the system at several temperatures over the full operational temperature range of 10-40 $^{\circ}$C.

Shutter

Shutters are used to prevent incoming optical radiation from entering into the instrument's photosensitive areas. The resulting measurement will therefore be an indication of the sum of the noise inherent in the radiometer and the perturbations caused by the physical environment, also known as a dark measurement. Subtracting this dark signal from a measurement taken with the shutter open will produce the true signature of the input radiance albeit uncalibrated.

The absence of a shutter in the prototype technology leads to the obvious problem of not being able to separate background signal from the true signal. A temperature dependant calibration of the instrument allows for the dark signal to be characterised as a function of temperature, allowing for dark signal to be subtracted manually post-capturing of data.

CONCLUSIONS

The prototype radiometer HyDROW exhibited above average performance in an optically dynamic medium. Results are envisaged to improve with post processing techniques to cater for straylight and self shadowing.

The performance capabilities of two candidate spectrometer cores (C1 and C2) were tested with the aim of integrating the best performing spectrometer module into a low-cost prototype radiometric device to be used for in-water applications. Strategically selected figures of merit formed the basis for comparison. C1, the less expensive of the two spectrometers has produced superior SNR, optical throughput and spectral sensitivity results making it the preferred candidate for use in the development of the prototype radiometer. The resulting instrument will be thoroughly calibrated in the laboratory before being deployed in an uncontrolled environment where its performance will tested and compared to that of a calibrated commercially purchased in-water radiometer.

The Loskop Dam, with its spatially diverse optical turbidity, has been a convenient environment to test the radiometric performance of the HyDROW in measuring in-water upwelling radiance. Differences relative to the reference instrument are at most 30 %. This performance compares well with results from similar radiometric comparisons. Moreover, the correlation between HyDROW and the reference is greater than 0.99 for most of the sites. It is expected that enhancements to the calibration procedures as well as further corrections for stray-light and shading will improve the relative comparison

BIBLIOGRAPHY

1. Bernard S. Research proposal on Safe Waters Earth Observation Sytems (SWEOS), CSIR, 2010 (Unpublished report)

2. Ramkilowan A, Chetty N, Lysko M and Griffith D. Performance Test of a Low Cost In-Water Radiometric Device at Loskop Dam, South Africa. UKZN and CSIR (DPSS), 2012 (Unpublished)

3. Diaby S. Economic impact of Neuse river closure on commercial fishing. North Carolina Division of Marine Fisheries, 1996 (Unpublished report)

4. Steidinger KA, Landsberg JH, Tomas CR and Burns JW. Harmful algal blooms in Florida. Harmful algal bloom task force technical advisory group, 1999.

5. Washington DC. Senate committee on Commerce, Science and Transportation. Report 105-357, 1998.

6. Nixon SW. Coastal marine eutrophication: A definition, social causes, and future concerns. OPHELIA, 1995; 41: 199-219

7. Dierssen H, Kudela RM, Ryan JP and Zimerman RC. Red and blacktides: Quantitative analysis of water-leaving radiance and perceived color for phytoplankton, colored dissolved organic matter, and suspended sediments. Limnology and Oceanography, 2000; 51(6): 2646–2659

8. Bowers DG, Smith PSD, Kratzer S, Morrison JR, Tett P, Walne AW, Wild-Allen K. On the calibration and use of in-situ ocean colour measurements for monitoring algal blooms. INt. J. Of remote sensing, 2010; 22(2): 359 – 368.

9. Bailey SW, Hooker SB, Antoine D, Franz BA, and Werdel PJ. Sources and assumptions for the vicarious calibration of ocean color satellite observations. J. of Applied Optics. 2008; 47(12): 2035-2045.

10. Werdel PJ, Bailey SW, Franz BA, Morel A and McClain CR. On-orbit vicarious calibration of ocean color sensors using an ocean surface reflectance model. J. of Applied Optics. 2007; 46(23): 5649-5666.Japan.

11. Eutrophication Monitoring Guidelines by Remote Sensing for the NOWPAP Region, NOWPAP Special Monitoring & Coastal Environmental Assessment Regional Centre (NOWPAP CEARAC), 2007.

12. Hooker SB, McClain CR and Mannino A. A Comprehensive Plan for the LongTerm Calibration and Validation of Oceanic Biogeochemical Satellite Data. NASA Center: Goddard Space Flight Center NASA SP-2007-214152. 2007.Cullen JJ, Ciotti AM, Davis RF and Lewis MR. Optical detection of algal blooms. Int. J Oceonog. 1997; 42 (5 pt 2): 1223-1239

13. Hooker SB, McClain CR and Mannino A. A Comprehensive Plan for the LongTerm Calibration and Validation of Oceanic Biogeochemical Satellite Data. NASA Center: Goddard Space Flight Center NASA SP-2007-214152. 2007.Cullen JJ, Ciotti AM, Davis RF and Lewis MR. Optical detection of algal blooms. Int. J Oceonog. 1997; 42 (5 pt 2): 1223-1239

14. Parliamentary Grant Deliverable-March 2008 State of the nation report An Overview of the Current Status of Water Quality and Eutrophication in South African Rivers and ReservoirsPaul J. Oberholster and Peter J. Ashton

15. Oberholster PJ, Claasen M, Cloete T E and Botha A M. Linking climate changes and eutrophication of surface water resources in South Africa to the occurrence of blue green algae blooms. Journal of African biotechnology. 2008; 8: 21

16. Hutchings L, Roberts M R and Verheye H M. Marine environmental monitoring programmes in South Africa: a review. South African Journal of Science. 2009;a: 105

17. Lysko M, Griffith D, Ramkilowan A and Govender P. SWEOS annual report. 2011 [unpublished]

18. Choi H. Advantages of a photodiode array. Manual SCINCO Co. Ltd and the references therein. Korea.

19. Robertson G.W. and Holmes R.M. A spectral Light Meter: Its Construction Calibration and Use. Ecological Society of America. Ecology, Vol 44, No 2 (Apr 1963). pp. 419-423

20. Venkataraman S and Deshmukh P C. 100 years of Einstein's photoelectric effect. Bulletin of Indian Physics Teachers Association. 2006.

21. Hamamatsu. Data and specifications sheet for mini-spectrometers. Japan. 2009

22. Hamamatsu. Ultra compact mini-spectrometer integrating MEMS and image sensor technologies. Japan. 2011.

23. Boehringer Ingelheim. Monolithic microspectrometer (OEM) for spectral sensing applications. Germany. 2005

24. Kohler D D R and Philpot W D. Comparing in situ and remotely sensed measurements in optically shallow waters. Ocean Optics XV. Monaco. 2000

25. Saber G. R. Salim, Nigel P. Fox, Evangelos Theocharous, Tong Sun, and Kenneth T. V. Grattan. Temperature and nonlinearity corrections for a photodiode array spectrometer used in the field. Applied Optics, Vol. 50, Issue 6, pp. 866-875. 2011

Paper II

HyDROW Performance Test at Loskop Dam

A. Ramkilowan, Dr N. Chetty, D. J. Griffith, Dr M. D. Lysko

Submitted to the Journal of Atmospheric and Oceanic Technology (11 February, 2012) and printed herein according to the prescribed template.

HyDROW Performance Test at Loskop Dam

Arshath Ramkilowan[1]
Council for Scientific and Industrial Research, Pretoria, South Africa

Naven Chetty
University of KwaZulu-Natal, South Africa

Derek J. Griffith
Council for Scientific and Industrial Research, Pretoria, South Africa

Meena D. Lysko
Council for Scientific and Industrial Research, Pretoria, South Africa

[1] *Corresponding author address*: Arshath Ramkilowan, CSIR DPSS, P O Box 395, Pretoria 0001, South Africa
E-mail: aramkilowan@csir.co.za

Abstract

South Africa's fresh water resources are under threat by Harmful Algal Blooms (HABs). A comprehensive and cost effective method for wide area detection and monitoring of HABs is therefore needed to manage and where possible circumvent the negative impact HABs may have on the country's aquatic ecosystems. Current commercial radiometers used for such applications are often too costly to purchase in numbers. This study focuses on the performance of a low cost, in-house developed prototype radiometer, **Hy**perspectral **D**evice for **R**adiometric **O**bservations in **W**ater (HyDROW). HyDROW's performance has been evaluated against data assimilated with a commercially available **Hyper**spectral **T**ethered **S**pectral **R**adiometer **B**uoy (HyperTSRB) during a field campaign at Loskop Dam in South Africa. The Loskop Dam is at risk for HABs and has been selected given its diverse environments from an optical perspective. Measurements were made at five optically diverse test points. The maximum percentage difference between the HyperTSRB and HyDROW were ~8% in the blue, ~19% in the green and ~24% in the red bands of the spectrum. The correlation coefficients between the radiometers range from 0.97 at the most turbid of test sites, to better than 0.99 in clearer waters.

1. Introduction

Safe Water Earth Observation Systems (SWEOS) is a multidisciplinary initiative which seeks to address the severe impact that Harmful Algal Blooms (HABs) have on water resources in South Africa. Ramkilowan et al. (2012), Bernard (2010) and Lysko et al. (2011) provide background on SWEOS. In gist, project SWEOS combines an innovative ensemble of remote sensing techniques with robust, cost effective and autonomous in-situ technology with the ultimate aim of providing a comprehensive and cost effective system for wide area detection and monitoring of the HABs in South Africa.

The development of economically priced bio-optical sensors is an invaluable facet of the project. A **Hy**perspectral **D**evice for **R**adiometric **O**bservations in **W**ater (HyDROW) has been developed based on selection criteria as discussed in (Ramkilowan et al., 2012). This study focuses on the performance evaluation of HyDROW for data quality assurance given the compromises shown in (Ramkilowan et al., 2012). In this study HyDROW's performance, as an in-water upwelling radiance sensor has been evaluated against data assimilated with a commercially available **Hyper**spectral **T**ethered **S**pectral **R**adiometer **B**uoy (HyperTSRB) during a field campaign on the Loskop Dam in South Africa.

2. Description of the Hyperspectral Radiometers

The tethered buoy for the HyperTSRB provided a convenient platform for co-located observations with HyDROW during the Loskop Dam campaign. The

coupling of the HyperTSRB and HyDROW gave both instruments the same viewing field which thereby reduced any scene bias.

HyperTSRB

The HyperTSRB system, from Satlantic, Inc., measures in-water upwelling radiance $Lu(\lambda_{400\ nm\ to\ 800\ nm}, z)$ at depth z = 0.66 m and downwelling irradiance $Ed(\lambda_{400\ nm\ to\ 800\ nm}, 0^{+}$ m) just above the water surface. Each radiometer has a 256 channel silicon photodiode array with pixel size 25 µm x 2500 µm. The spectrograph has a 70 µm x 2500 µm entrance slit and a 10 nm spectral resolution. Spectral sampling is at 3.3 nm/pixel. The full field of view in air and water are 3^{o} and 8^{o}, respectively. HyperTSRB compensates for thermal dark current changes that occur within the spectrograph with the use of a mechanical dark shutter that closes periodically in the radiometer. The HyperTSRB is configured with Satlantic's SatView application. SatView also logs the raw analogue to digital counts for subsequent conversion and post-processing. This work has used the Satlantic ProSoft 7.7.16 application for post-processing the raw counts to level 2 data. The level 2 data is calibrated and corrected with shutter dark readings and instrument immersion mode.

HyDROW

HyDROW is a prototype developed by the Council for Scientific and Industrial Research (CSIR). (Ramkilowan et al., 2012) have addressed the choice of spectrometer core for the radiometer. An optimized performance together with cost efficiency and field ruggedness had to be considered when deciding on the system electronics and radiometer housing. In gist,

HyDROW's core is a miniaturised spectrometer with a linear 256 pixel CMOS array. Each pixel size is 12.5 µm x 1000 µm. The spectrometer entrance slit is 75 µm x 750 µm. The spectral response range is 340 nm to 750 nm and the spectral resolution is 10 nm. Together with fore-optic coupling, HyDROW has an 8^{o} full field of view in water.

The absence of a shutter in the prototype technology leads to the obvious problem of not being able to separate background signal from the true signal. A temperature dependant calibration of the instrument allows for the dark signal to be characterised as a function of temperature, allowing for dark signal to be subtracted manually post-capturing of data.

3. HyDROW Calibration

HyDROW has been designed for in-water applications, which may include mooring at a permanent or semi-permanent site. For such cases prolonged exposure to sunlight, rough tides, natural contaminants and vandalism may threaten the reliability and consistency of the instrument data. It is therefore necessary for the radiometer to be frequently calibrated. The conventional and in-lab approach for calibration of radiometers is with a calibrated radiometer together with a uniform and well defined light source having good spectral balance to characterise the response of the instrument. To calibrate the instrument on a regular basis in this manner is not feasible. Instead a clear blue sky supplemented with the relevant aerosol optical parameters and a field type reference radiometer can be used. The blue sky which is as a result of Rayleigh scattering offers sufficient spectral range for calibration of an instrument in the visible portion of the electromagnetic spectrum. An

obvious advantage of this method of calibration is that it allows for on-site calibration, provided weather conditions are suitable and that the aerosol and molecular content is simultaneously mapped.

4. Sample Sites

Sample sites on the Loskop Dam were determined primarily with two criteria: a) representation of various regions, and b) representation of various optical water types in the lake.

Loskop Dam is located in Mpumalanga province about 100 km northeast of the city, Pretoria (25.43^{o}S, 29.34^{o}E). It is a single water body with pronounced changes in turbidity levels along its length as evident from (Oberholster et al., 2009) and (Oberholster et al., 2012). Optically turbid zones have been found near the river inlet, with progressively clearer waters closer to the main basin. This optical turbidity range within a single water body is uncommon and has provided the basis to probe HyDROW's quality, accuracy and reliability across a dynamic turbidity range.

Five sample sites were selected along the length of the dam as shown in Fig. 1. The environment condition per site is given in the Table 1. The range of Secchi disk depths (Table 1), measured during the field trial, is an indication of variation in optical turbidity.

5. Data Capturing Methodology

The Loskop Dam field data for this comparison was collected on 8 August 2011. The HyperTSRB's tethered mooring provided the ideal platform as HyDROW could be secured side by side with the upwelling radiance sensor

of the HyperTSRB. Special effort was put into ensuring that neither radiometer had a compromised field of view. The norm, as shown in (Mueller, 2003) and (Barker, 2011) is to allow the buoy to sit at the water surface a distance of at least 30 m from the boat. The buoy was hand-deployed during the campaign and was therefore within 1 m from the boat. A concerted effort was made to ensure that no bubbles collected at the water-lens interface and that shadowing from the boat and the moored system itself was negated as far as possible.

To be able to interpret the data captured from the HyDROW, HyperTSRB reference radiometric data was captured simultaneously. Data sets were acquired in 3 minute bursts with exposure times ranging from 250 to 1000 ms. The user defined exposure time for HyDROW was chosen so as to be within 1 ms of the optimised exposure time set by HyperTSRB. Between 100 and 200 samples per wavelength were averaged to account for the waters inherent optical variability. Secchi disk readings were taken at each sample site and allowed for a relationship to be formed between the performance of HyDROW and the clarity of a given water sample.

6. Data Comparison

The Lu(λ,0.66 m) spectra from both HyperTSRB and HyDROW are relatively constant in shape (see Fig. 2) for four of the sample sites: Buoy, Lacustrine, Main Basin and River Inlet. The data from Ceratium is plotted separately in Fig.3. A large relative standard deviation (RSD) for this site is expected given the significant optical turbidity with the higher concentration of

phytoplankton. The distinct step feature at about 590 nm and the sharp peak at 725 nm is followed by both the unit under test and the reference.

The relative deviation plots from the second column in Fig. 2. show that disagreement between HyperTSRB and HyDROW is below 10 % between 450 nm and 550 nm and within 30 % for wavelengths exceeding 550 nm.

The correlation between Lu_{HyDROW} (λ,0.66 m) and $Lu_{HyperTSRB}$ (λ,0.66 m) for each sample site has been calculated using the Pearson's product moment correlation coefficient *r* (Bhattacharyya et al., 1977). That is:

$$r = \frac{\sum_{i=1}^{n} \left(X_i - \overline{X}\right)\left(Y_i - \overline{Y}\right)}{\sqrt{\left[\sum_{i=1}^{n} \left(X_i - \overline{X}\right)^2\right]\left[\sum_{i=1}^{n} \left(Y_i - \overline{Y}\right)^2\right]}}, \quad (1)$$

where (X_1,Y_1), … (X_n,Y_n) are the *n* pairs of observations. It is seen from TABLE 2 that *r* is above 0.99 for all sample sites except for Ceratium (r = 0.97). As expected, *r* also increases as the water clarity increases.

7. Considered Error Factors

Accurate in-water radiometric measurements in an uncontrolled environment are a challenge. The instrument design, calibration, measurement protocol and errors associated with environmental effects contribute to large measurement uncertainties. As an example, (Hooker, 2000) reports an in-water up-welling radiance Lu(z = depth down to 1 % light level, 510 nm) deviation of up to 25 % between two radiance profilers that were deployed by winch. Much effort has therefore been made to identify and decrease uncertainties. It is noted that the advancement of optical instrumentation technology and studies such as (Leathers et al., 2001), (Torrecilla et al., 2008) and (Ohde et al., 2003) address the most significant sources of

radiometric uncertainty in measurements of Lu(z, λ) and suggest methods to investigate and reduce errors due to instrument self-shading, tilt, stray light, immersion and depth differences.

Immersion factors

When a light detecting device is used in a medium different to that in which it was calibrated, the change in refractive index of the intervening medium (in this case water) causes alterations in absolute spectral response. An immersion factor I_f is used to compensate for the difference in response of the instrument. Two effects influence in-water radiance measurements. Firstly the refractive index at glass-air interface (during calibration) differs from the refractive index of the glass-water interface (during in-water measurements). Secondly when submerged in water the field of view solid angle of the instrument is reduced allowing a smaller percentage of the radiance to be detected. (Ohde et al., 2003) references an equation for the wavelength dependant immersion factor

$$I_f(\lambda) = \frac{n_w(\lambda)[n_w(\lambda) + n_g(\lambda)]^2}{(1 + n_g(\lambda))^2} \quad (2)$$

Here n_w is the refractive index of the water and n_g is the refractive index of the glass window of the instrument. The wavelength dependence of n_g can be calculated from the Sellmeier equation:

$$n_g{}^2 = 1 + \frac{B_1\lambda^2}{\lambda^2 - C_1} + \frac{B_2\lambda^2}{\lambda^2 - C_2} + \frac{B_3\lambda^2}{\lambda^2 - C_3}, \quad (3)$$

where the coefficients are the experimentally determined Sellmeier coefficients given in TABLE 3.

The freshwater system in which HyDROW was tested consisted of organic assemblages which made n_w a variable quantity. Given that the purpose of this research was to measure the instrument's relative and not absolute performance, the consistent value of n_w = 1.345 employed for fresh water by the reference radiometer was adopted. The fundamental changes in refractive index due to temperature fluctuations are noted and estimated to contribute less than 1% over the operational temperatures. While n_w is likely to differ from the true index of refraction of the water, the consistent use of it for both instruments reduce the relative error.

Self-shading

The contribution of self-shading to an immersed radiometer is dependent on the geometry of the radiometer and platform, the absorption coefficient of the medium, the Sun zenith and the atmospheric turbidity. It is noted that average self-shading errors for the upwelling radiance of the HyperTSRB is about 5 % (Leathers et al., 2001). However, as a system, Lu_{HyDROW} (λ,0.66 m) relative to $Lu_{HyperTSRB}$ (λ,0.66 m) is not expected to have a significant bias due to self-shading since both instruments are strapped under the same bouy such that the differential effect of shadowing due to the buoy would be minimal. In this study, self-shading for the individual instruments has not been corrected for.

Stray-light

The high spectral resolution of hyperspectral radiometers provides the advantage to discern a target's fine-scale spectral features. The spectral selection in systems such as HyperTSRB and HyDROW is accomplished with

a fixed dispersive optical train. The upwelling radiance signature is captured as an image of the entrance slit onto the detector array. Ideally, the image should be consistent with the spectral components of the target, within the instrument's bandpass. In practice, the imaged signature may be modified due to radiation from out-of-band wavelengths which activates a signal at the detector element. The modification is seen as instrumental stray-light. The sources of instrumental stray-light include ambient light distribution, scattered light from imperfect optical components, reflections off non-optical components and overlap from multiple order diffraction. Stray-light may cause the measured upwelling radiance to be erroneously high.

As shown in (Satlantic Inc., 2008), stray-light contribution to $Lu_{HyperTSRB}(\lambda,z)$ can be up to 2 orders of magnitude higher than the true signal in extreme cases. With stray-light correction, stray-light contribution can be reduced to less than 0.2% (for 450 nm to 800 nm) and less than 2 % (for 350 nm to 450 nm). It is noted that $Lu_{HyperTSRB}(\lambda,0.66\ m)$ data from the Loskop Dam campaign is not stray-light corrected. This can be done after a re-calibration of the HyperTSRB and with data processed with ProSoft 8.0.

Instrument stray-light can be resolved by using sufficiently narrow spectral band sources with sufficient output power (Zong et al., 2006). This approach is not always practical. A selection of spectral cut-on filters against a uniform broad-band light source has been used to gauge the stray-light performance of HyDROW. For each filter, the net signal below the cut-on wavelength is considered as stray-light. Net stray-light was found to be less than 5 % with each of the cut-on filters (see TABLE 4). The limited set of cut-on filters does not allow for a complete characterisation of HyDROW for

stray-light. $Lu_{HyDROW}(\lambda,0.66\ m)$ data from the Loskop Dam campaign is therefore not stray-light corrected.

8. Summary

The Loskop Dam, with its spatially diverse optical turbidity, has been a convenient environment to test the radiometric performance of the HyDROW in measuring in-water upwelling radiance. Differences relative to the reference instrument are at most 30 %. This performance compares well with results from similar radiometric comparisons. Moreover, the correlation between HyDROW and the reference is greater than 0.99 for most of the sites. It is expected that enhancements to the calibration procedures as well as further corrections for stray-light and shading will improve the relative comparison.

References

1. Barker, K., (2011): MERIS Optical Measurement Protocols. Part A: In-situ water reflectance measurements. CO-SCI-ARG-TN-008, retrieved from http://hermes.acri.fr/mermaid/dataproto on 2012-02-07.
2. Bhattacharyya G. K., R. A. Johnson, (1977): Statistical concepts and methods. John Wiley & Sons, USA.
3. Frette, Ø., J. J. Stamnes and K. Stamnes, (1998): Optical Remote Sensing of Marine Constituents in Coastal Waters: A Feasibility Study, *Applied Optics*, Vol. 37, Issue **36**, 8318-8326.
4. Hooker, S. B. and S. Maritorena, (2000): An Evaluation of Oceanographic Radiometers and Deployment Methodologies, *J. Atmos. Oceanic Technol.*, **17**, 811-830.
5. Leathers, R. A., T. V. Downes, C. D. Mobley (2001): Self-shading correction for upwelling sea-surface radiance measurements made with buoyed instruments. *Optics Express*, Vol. 8, No. **10**, 561-570.
6. Lysko, M. D., D. J. Griffith, A. Ramkilowan and P. Govender (2011): SWEOS annual report. **CSIR**, 6700-SWEOS-59520-01, (unpublished report).
7. Mueller, J. L., G. S. Fargion and C. R. McClain, (2003): Ocean Optics Protocols For Satellite Ocean Color Sensor Validation, Revision 4, Volume VI: Special Topics in Ocean Optics Protocols and Appendices. NASA/TM-2003-211621/Rev4-Vol.VI.
8. Oberholster, P. J., J. G. Myburgh, P. J. Ashton, A.-M. Botha, (2009): Responses of phytoplankton upon exposure to a mixture of acid mine

drainage and high levels of nutrient pollution in Lake Loskop, South Africa. *Ecotoxicology and Environmental Safety*, **73**, 326–335.

9. Oberholster, P. J., J. G. Myburgh, P. J. Ashton, J. J. Coetzee, and A-M. Botha, (2012): Bioaccumulation of aluminium and iron in the food chain of Lake Loskop, South Africa. Ecotoxicology and Environmental Safety, **75**, 134–141.
10. Ohde, T. and H Siegel, (2003): Derivation of immersion factors for the hyperspectral TriOS radiance sensor, *J. Opt. A: Pure Appl*. **Opt. 5**, L12–L14.
11. Ramkilowan, A., N. Chetty, D. J. Griffith and M. D. Lysko, (2012, under review): Optical Detectors for Integration into a Low Cost Radiometric Device for In-Water Applications: A Feasibility Study. S Afr J Sci.
12. S. Bernard, (2010): Research proposal on Safe Waters Earth Observation Systems (SWEOS), **CSIR**, (unpublished report).
13. Satlantic Incorporated, (2008): ProSoft 8.0 User Manual. Document Number: SAT-DN-00228, Revision: 8.0B.
14. SCHOTT, (2011): Optical glass data sheet.
15. Torrecilla, E., S. Pons, M. Vilaseca, J. Piera, J. Pujol, (2008): Stray-light correction of in-water array spectroradiometers. Effects on underwater optical. *IEEE OCEANS 2008*, 1-7.
16. Zong, Y., S. W. Brown, B. C. Johnson, K.R. Lykke and Y. Ohno, (2006): A Simple Stray-light Correction Method for Array Spectroradiometers, *Applied Optics*, Vol. **45**, Issue **6**, 1111-1119.

List of Tables

List of Figures

TABLE 1. Environment conditions at sample sites on 8 August 2011.

	River Inlet	Ceratium	Buoy	Lacustrine	Main Basin
Location	25.495°S, 29.245°E	25.488°S, 29.264°E	25.465°S, 29.259°E	25.468°S, 29.279°E	25.430°S, 29.323°E
Site arrival time GMT+2	09H00	09H40	10H30	11H00	11H30
Wind	3.0 mph NW	5.5 mph SW	4.5 mph SW	2.5 mph NE	None
Wave height	~ 1 cm	~ 2 cm	~ 2 cm	~ 2 cm	~ 1 cm
Cloud cover	~ 75 %	< 10 %	< 10 %	< 10 %	< 10 %
Mean Secchi disk depth	193 cm	45 cm	325 cm	438	654 cm

TABLE 2. Correlation between HyDROW and TSRB and relation to mean Secchi disk depth.

	Main Basin	Lacustrine	Buoy	River Inlet	Ceratium
Mean Secchi disk depth	654 cm	438	325 cm	193 cm	45 cm
Correlation coefficient, *r*	0.9946	0.9948	0.9921	0.9905	0.9744

TABLE 3. Constants of dispersion for equation (3) to determine HyDROW's I_f.

	Sellmeier co-efficients (Schott, 2011)
B1	1.03961212
B2	0.231792344
B3	1.01046945
C1	0.00600069867
C2	0.0200179144
C3	103.560653

TABLE 4. HyDROW net stray-light for 3 cut-on filters.

Filter Cut-on Wavelength	Net Stray-Light
517 nm	0.5 %
622 nm	1.9 %
667 nm	4.2 %

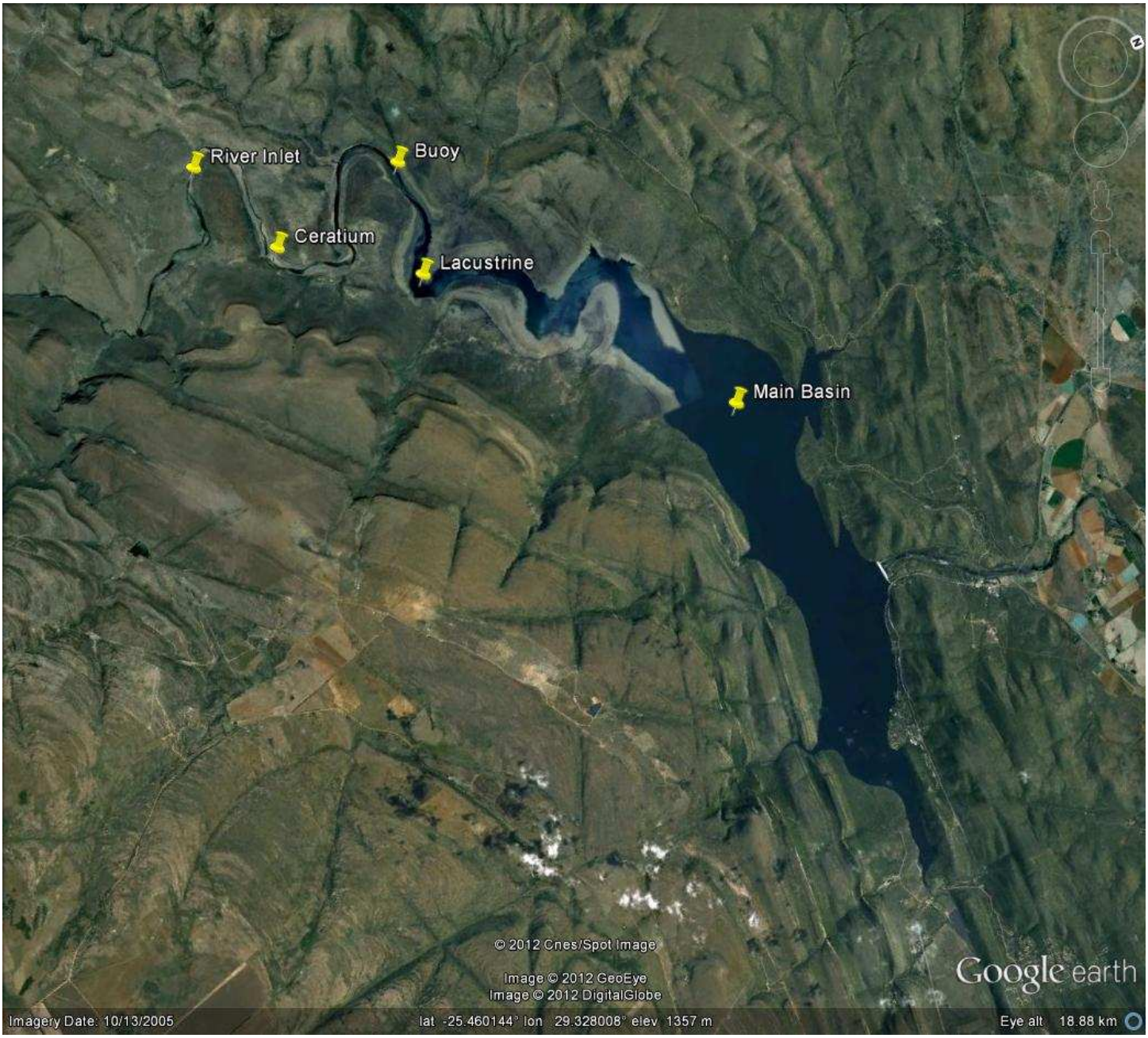

FIG. 1. Google Earth image over Loskop Dam with the five sample sites.

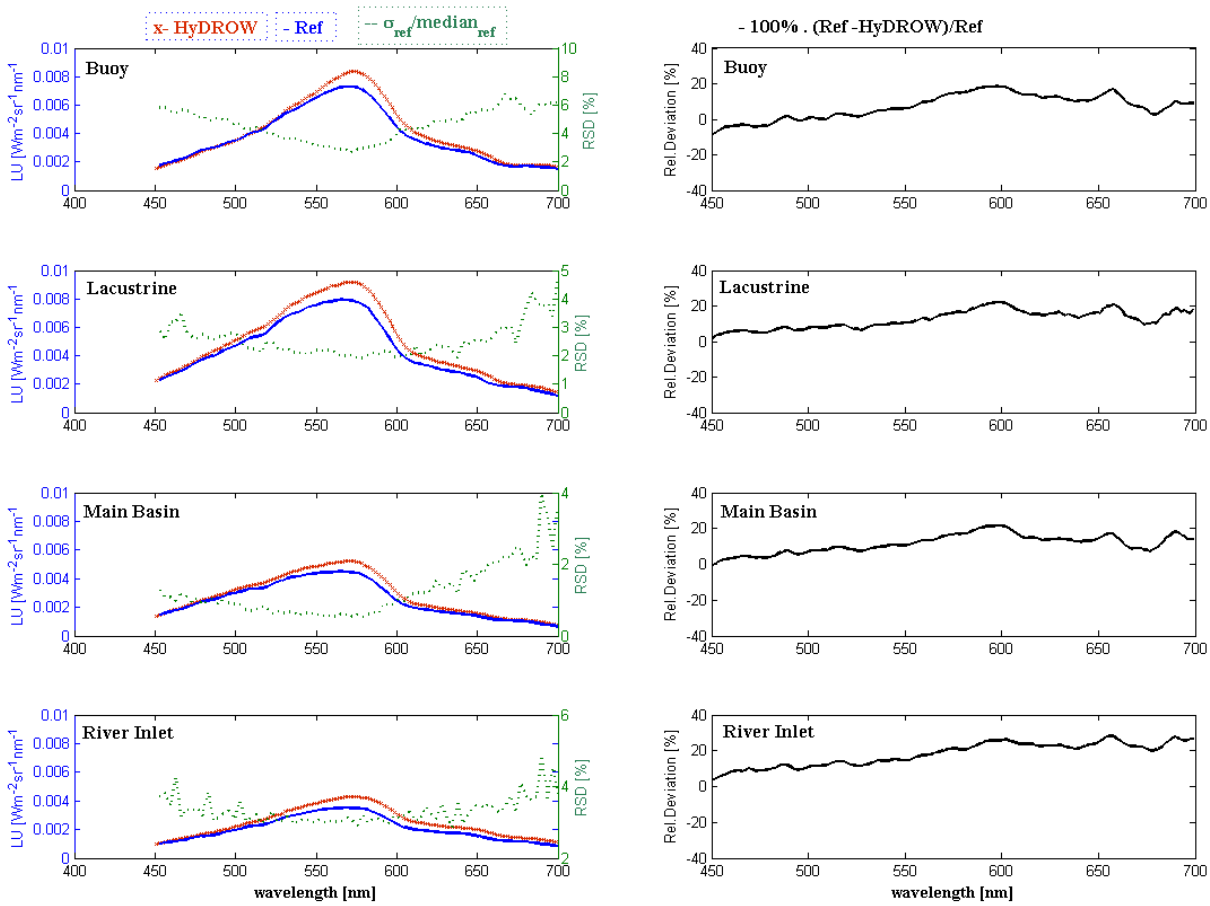

FIG. 2. Column1: Lu(λ, 0.66 m) from HyperTSRB and HyDROW per sample site, with the RSD from HyperTSRB. Column2: HyDROW Lu(λ, 0.66 m) deviation relative to HyperTSRB.

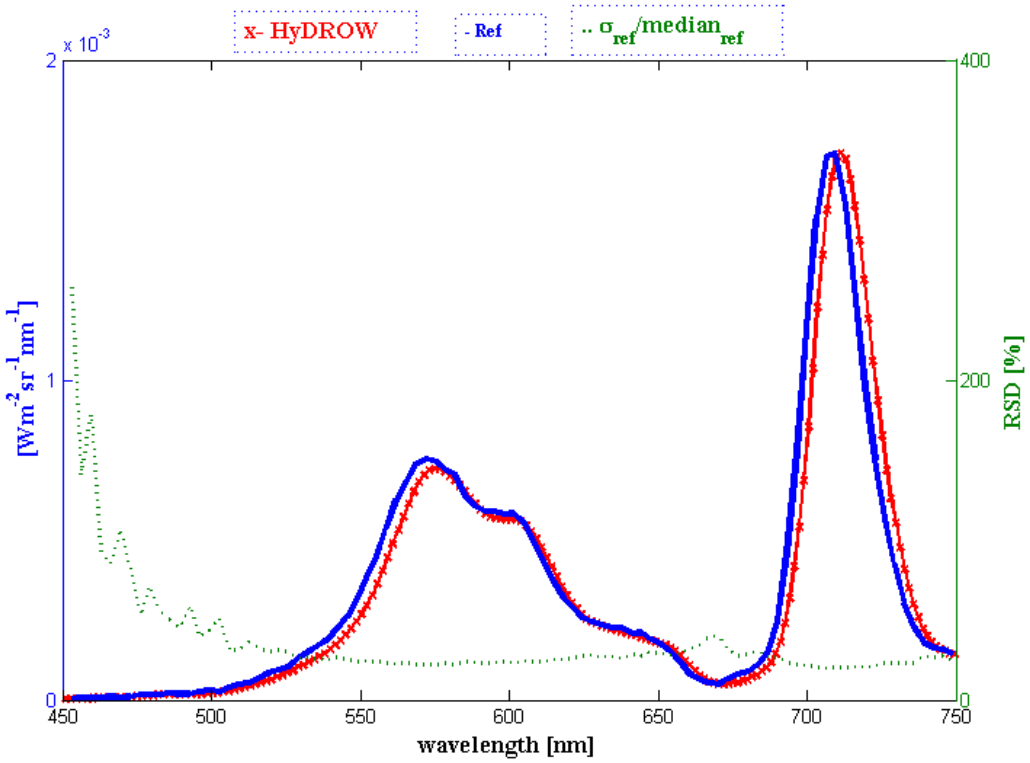

FIG. 3. Lu(λ, 0.66 m) from HyperTSRB and HyDROW at sample site Ceratium, with the RSD from HyperTSRB.